地层学杂志, 2021 年 3 月, 45(1): 69-81

科学出版社

地层学杂志

JOURNAL OF STRATIGRAPHY

http://www.dcxz.cbpt.cnki.net

中文引用格式: 史恭乐, 李建国, 谭覃, 董重, 李秋立, 吴琼, 章伯乐, 尹素心, HERRERA Fabiany, HERENDEEN Patrick S., CRANE Peter R. 2021. 内蒙古东部霍林河盆地霍林河组的年龄: 来自锆石 U-Pb 测年和孢粉组合的证据. 地层学杂志, 45(1): 69-81. DOI: 10.19839/j.cnki.dcxzz.2021.0001.

英文引用格式: Shi G L, Li J G, Tan T, Dong C, Li Q L, Wu Q, Zhang B L, Yin S X, Herrera F, Herendeen P S, Crane P R. 2021. Age of the Huolinhe Formation in the Huolinhe Basin, eastern Inner Mongolia, China: Evidence from U-Pb zircon dating and palynological assemblages. Journal of Stratigraphy, 45(1): 69-81. DOI: 10.19839/j.cnki.dcxzz.2021.0001.

内蒙古东部霍林河盆地霍林河组的年龄: 来自锆石 U-Pb 测年和孢粉组合的证据①

史恭乐 1)2)　李建国 1)2)3)　谭 覃 1)2)3)　董 重 1)2)　李秋立 4)3)　吴 琼 5)　章伯乐 6)　尹素心 1)2)3)

HERRERA Fabiany 7)　HERENDEEN Patrick S. 7)　CRANE Peter R. 8)9)

1) 中国科学院南京地质古生物研究所, 现代古生物学和地层学国家重点实验室　江苏南京　210008;

2) 中国科学院生物演化与环境卓越创新中心　江苏南京　210008;

3) 中国科学院大学　北京　100049;

4) 中国科学院地质与地球物理研究所, 岩石圈演化国家重点实验室　北京　100029;

5) 南京大学地球科学与工程学院　江苏南京　210023;

6) 青岛市勘察测绘研究院　山东青岛　266030;

7) 芝加哥植物园, Glencoe, 伊利诺伊 60022, 美国;

8) 耶鲁大学环境学院, 纽黑文, 康涅狄格 06511, 美国;

9) 橡树泉园林基金会, Upperville, 弗吉尼亚 20184, 美国

摘　要: 内蒙古东部霍林河盆地霍林河组是我国最重要的下白垩统含煤地层之一。该组产出大量不同种类且保存完好的植物化石, 但因为缺乏海相沉积和火山岩夹层, 我们对这套地层的精确年龄认知不足。我们最近在扎鲁特旗扎哈淖尔露天煤矿霍林河组发现了火山灰层, 基于钻孔数据的地层分析显示该火山灰层位于霍林河组下含煤段的底部。二次离子质谱(SIMS)锆石 U-Pb 年代学研究得出的该火山灰层沉积年龄为 125.6±1.0 Ma (巴雷姆期晚期–阿普特期最早期), 这一结果与激光剥蚀-等离子体质谱(LA-ICP-MS)对同一样品分析得出的年龄一致。火山灰层保存的孢粉化石组合以裸子植物花粉和蕨类及苔藓的孢子为主, 被子植物花粉非常稀少, 且仅有棒纹粉 *Clavatipollenites* 一种。这一孢粉组合支持火山灰层的年龄为巴雷姆期晚期至阿普特期最早期。本研究为认识整个霍林河组的年龄及火山灰层上覆地层保存的重要植物化石的最大年龄提供了重要数据。

关 键 词: 霍林河组, 早白垩世, 含煤盆地, U-Pb 地质年代学, 孢子花粉, 内蒙古

中图分类号: P534.53　　**文献标识码:** A　　**文章编码:** 0253-4959(2021)01-0069-13

① 中国科学院战略性先导科技专项(B 类)(XDB26000000)、国家自然科学基金(41790454、41802014、41772014)、美国国家科学基金(DEB-1748286)和中国科学院青年创新促进会(2017359)共同资助。

文稿接受日期: 2021-02-03; 修改稿收到日期: 2021-02-07

通信作者简介: 史恭乐, 研究员, 主要从事古植物学和植物演化生物学研究; e-mail: glshi@nigpas.ac.cn

AGE OF THE HUOLINHE FORMATION IN THE HUOLINHE BASIN, EASTERN INNER MONGOLIA, CHINA: EVIDENCE FROM U-Pb ZIRCON DATING AND PALYNOLOGICAL ASSEMBLAGES

SHI Gong Le [1)2)], LI Jian Guo [1)2)3)], TAN Tan [1)2)3)], DONG Chong [1)2)], LI Qiu Li [4)3)], WU Qiong [5)], ZHANG Bo Le [6)], YIN Su Xin [1)2)3)], HERRERA Fabiany [7)], HERENDEEN Patrick S. [7)], CRANE Peter R. [8)9)]

1) *State Key Laboratory of Palaeobiology and Stratigraphy*, *Nanjing Institute of Geology and Palaeontology*, *Chinese Academy of Sciences*, *Nanjing* 210008;
2) *Center for Excellence in Life and Paleoenvironment*, *Chinese Academy of Sciences*, *Nanjing* 210008;
3) *University of Chinese Academy of Sciences*, *Beijing* 100049;
4) *State Key Laboratory of Lithospheric Evolution*, *Institute of Geology and Geophysics*, *Chinese Academy of Sciences*, *Beijing* 100029;
5) *School of Earth Sciences and Engineering*, *Nanjing University*, *Nanjing* 210023;
6) *Qingdao Research Institute of Geotechnical Prospecting and Surveying*, *Qingdao* 266030;
7) *Chicago Botanic Garden*, *Glencoe*, *IL* 60022, *USA*;
8) *Yale School of the Environment*, *Yale University*, *New Haven*, *CT* 06511, *USA*;
9) *Oak Spring Garden Foundation*, *Upperville*, *VA* 20184, *USA*

Abstract The Huolinhe Formation in the Huolinhe Basin, eastern Inner Mongolia is one of the most important Lower Cretaceous coal-bearing strata in China, yielding abundant, diverse, and well-preserved plant fossils. Its precise age, however, is poorly known due to lack of associated marine deposits and volcanic beds. Here we present U-Pb zircon ages, and the associated palynological assemblages of an ash layer of the Huolinhe Formation recently discovered at the Zhahanaoer open-cast coal mine in Jarud Banner. Stratigraphic analyses based on boreholes suggest that the ash layer occurs near the bottom of the "lower coal-bearing member" of the Huolinhe Formation. U-Pb zircon geochronology using the SIMS method constrains the depositional age of the ash layer to be 125.6±1.0 Ma (late Barremian–earliest Aptian), and this is consistent with the result from LA-ICP-MS analyses of the same sample. A late Barremian–earliest Aptian age for the ash layer is also supported by the palynological assemblage associated with the layer, in which the pollen of gymnosperms and the spores of ferns and bryophytes are dominant, angiosperm pollen is very rare and represented by only *Clavatipollenites*. This study contributes important new data for understanding the age of the entire Huolinhe Formation and also provides a more precise maximum age for the key plant fossils preserved in the deposits above the ash layer.

Key words Huolinhe Formation, Early Cretaceous, coal-bearing basin, U-Pb geochronology, pollen and spores, Inner Mongolia

1 Introduction

The Huolinhe Formation is a Lower Cretaceous terrestrial coal-bearing unit distributed in the Huolinhe Basin, one of several important coal-bearing, fault-bounded basins formed during Late Jurassic and Early Cretaceous in the region of the Greater Khingan Range in northeastern China (Li *et al.*, 1982). The Huolinhe Basin in Jarud Banner, eastern Inner Mongolia is ~60 km long and ~9 km wide and is oriented along a northeast to southwest line. Within the basin the Huolinhe Formation rests unconformably on the Upper Jurassic volcanic Xing'anling Group, and comprises a sequence of terrestrial and fluvio-lacustrine-swamp sediments that are up to 1700 m thick (Li *et al.*, 1982). The formation is composed of conglomerate, sandstone, siltstone, mudstone, as well as thick coal and lignite seams. In ascending order the Huolinhe Formation is divided informally into a "conglomerate-sandstone member", a "lower mudstone member", a "lower coal-bearing member", an "upper mudstone member", an "upper coal-bearing member", and a "top mudstone member" (Li *et al.*, 1982). Most of the exploitable coal/lignite seams are in the "lower coal-bearing member", which is up to 720 m thick and has yielded abundant well-preserved plant megafossils (Deng, 1995).

The Huolinhe Basin is among the most extensively studied areas for Mesozoic plant fossils in China (Sun, 1987, 1993; Sun & Shang, 1988; Chen & Deng, 1990; Deng, 1991, 1995, 1997; Mei & Cui, 1994; Cui, 1995; Guo, 1995; Sun *et al.*, 2003; Dong & Sun, 2012; Xu *et al.*, 2013, 2017; Li *et al.*, 2014, 2016, 2021; Guignard, 2019). The plant fossil assemblage from the "lower coal-bearing member" of the Huolinhe Formation is diverse and dominated by ferns, including bryophytes, lichens, Lycopodiales, Equisetales, Filicales, Cycadales, Ginkgoales, Bennettitales, Coniferales and Czekanowskiales, along with some seeds and cones of uncertain affinity (Deng, 1995). No angiosperm megafossils have been reported so far. The floral composition suggests an early Early Cretaceous age, most probably Valanginian to early Hauterivian for the "lower coal-bearing member" of the Huolinhe Formation (Deng, 1995). However, more precise age constraints from the radioisotopic analyses have not been obtained for the Huolinhe Formation so far.

During recent fieldwork in the Huolinhe Basin, we identified an ash layer near the bottom of the "lower coal-bearing member" of the Huolinhe Formation at the Zhahanaoer open-cast coal mine in Jarud Banner. Here we report the U-Pb zircon ages for the ash layer and the associated palynological assemblages.

2 Material and methods

2.1 *Locality*

The ash samples for U-Pb zircon geochronology (059-2b, 059-2c) were collected at an outcrop exposed on the margin of the Zhahanaoer open-cast coal mine (45°21′38.5″N, 119°25′04″E), Jarud Banner, eastern Inner Mongolia, China. Boreholes and stratigraphic analyses suggest that the ash layer occurs below a considerable thickness of coal toward the bottom of the "lower coal-bearing member". The investigated section is ca. 11 m thick and composed of mudstone, silty mudstone, carbonaceous mudstone, siltstone, ash, and chert (Fig. 1). We divided the section into six units based on lithological features, and each of the six units was sampled for palynological analysis with sample numbers 059-1~059-6.

2.2 *Zircon preparation*

The zircon grains were separated using conventional techniques of heavy liquid separation and magnetic separation after ash samples were crushed and sieved. The grains for U-Pb isotopic analyses were selected by hand-picking under a binocular microscope, mounted in a transparent epoxy disk, and then polished to expose the interior of crystals for analyses. All zircon grains were photographed with transmitted and reflected light photo-microscopy and cathodoluminescence (CL) images to reveal their internal structure (Fig. 2) (Rubatto & Gebauer, 2000). The selected grains were analyzed with the Secondary Ion Mass Spectrometry (SIMS) and Laser Ablation Inductively Coupled Mass Spectrometer (LA-ICP-MS) techniques.

2.3 *U-Pb SIMS Geochronology*

Measurements of U-Pb zircon age by SIMS were conducted with a Cameca IMS-1280 ion microprobe at the Institute of Geology and Geophysics, Chinese Academy of Sciences (CAS) in Beijing, China. Details of the analysis and data-processing methods were described in Li *et al.* (2009, 2010). The zircon mount was vacuum-coated with high purity gold before SIMS measurements. During the analyses, the primary O_2^- ion beam was accelerated at 13 kV, with an intensity of ~10 nA and an analysis spot size of 20 μm × 30 μm. The mass resolution used to measure Pb/Pb and Pb/U isotopic ratios was 5400. U-Th-Pb ratios were determined relative to the standard zircon Plešovice (337.13±0.37 Ma, Sláma *et al.*, 2008), and the absolute abundances of U/Th were determined relative to standard zircon 91500 (Wiedenbeck *et al.*, 1995). Uncertainties for individual analyses are reported at a 1σ level; mean ages for pooled U/Pb and Pb/Pb analyses are quoted with 95% confidence intervals. To monitor the external uncertainties of SIMS U-Pb zircon dating, a standard Qinghu zircon was alternately analyzed as an unknown. Fourteen analyses on the Qinghu zircon produced a Concordia age of 160.7±1.1 Ma (MSWD = 0.94, n = 14), which is within the error range of the recommended ID-TIMS Concordia value of 159.5±0.2 Ma (Li *et al.*, 2013). The age calculation was made using Isoplot/Ex_ver3 at 95% confidence (Ludwig, 2003).

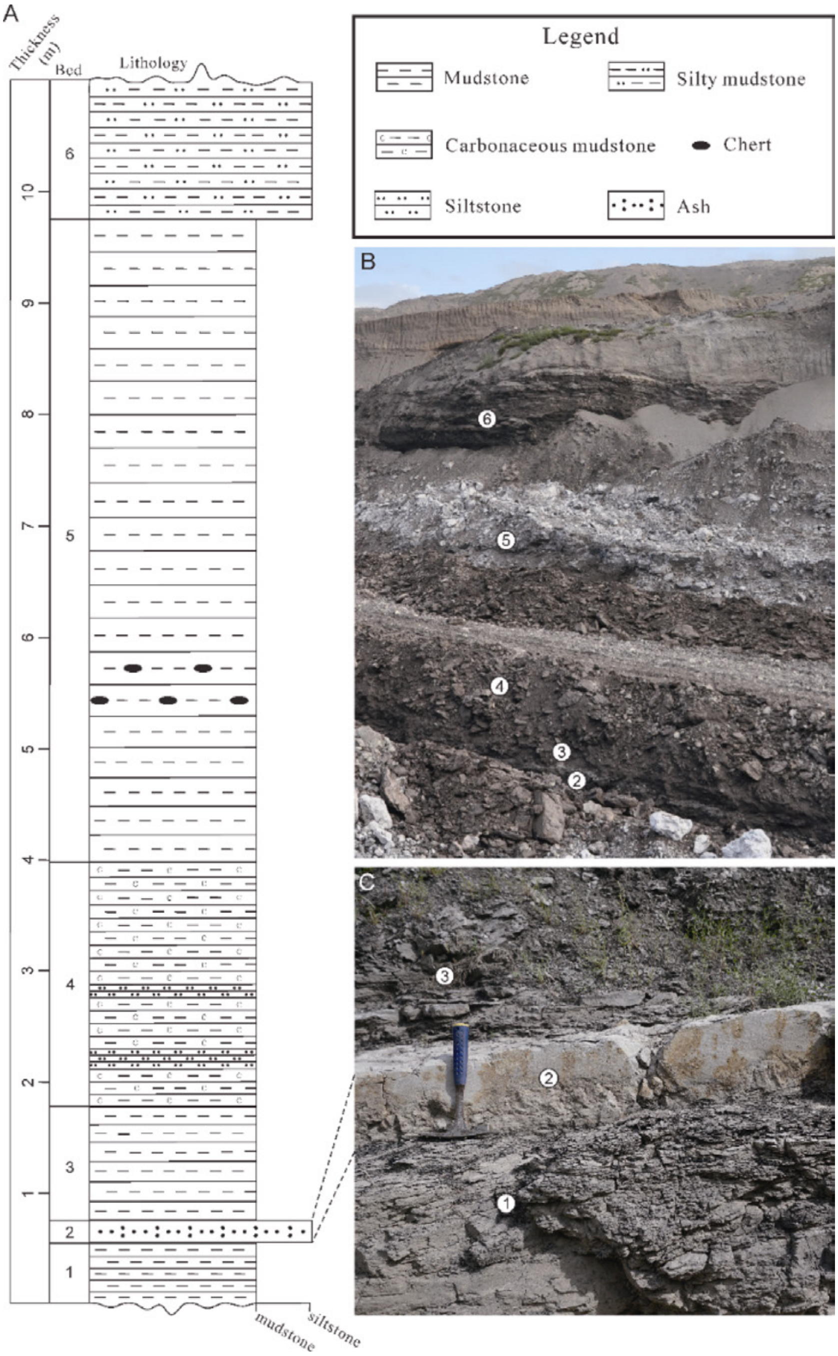

A– Stratigraphic column showing the lithology and the stratigraphic position of the ash layer for U-Pb zircon dating. The section is divided into six units based on lithological features, each of the six units were sampled for palynological analyses. B– Photograph of the outcrop with units 2–6 indicated by their numbers. C– Detail of the ash layer with units 1–3 indicated by their numbers

Fig. 1 The studied section of the "lower coal-bearing member" of the Huolinhe Formation at the margin of the Zhahanaoer coal mine in Jarud Bannar in eastern Inner Mongolia, China

2.4 *U-Pb LA-ICP-MS Geochronology*

Measurements of U-Pb zircon age by LA-ICP-MS were conducted at the Wuhan Sample Solution Analytical Technology Co., Ltd. in Wuhan, China. Details of the analyses and data-processing are described in Zong *et al.* (2017). Laser sampling was conducted using a GeolasPro laser ablation system that is composed of a COMPexPro 102 ArF excimer laser (wavelength of 193 nm and maximum energy of 200 mJ) and a MicroLas optical system. An Agilent 7700e ICP-MS instrument was used to acquire ion-signal intensities. Helium was applied as a carrier gas. Zircon 91500 (Wiedenbeck *et al.*, 1995) and glass NIST610 were used as external standards for U-Pb dating and trace element calibration respectively. Each analysis consisted of a background acquisition of (~)20~30 s followed by a further 50 s of data acquisition from the sample, with laser spot size of 32 μm and frequency of 5 Hz. Off-line data processing was performed using ICPMSDataCal software (Liu *et al.*, 2008). The age calculation was made using Isoplot/Ex_ver3 at 95% confidence (Ludwig, 2003).

2.5 *Palynological preparation*

The palynological samples were prepared using standard palynological techniques at the Experimental Technologies Center of Nanjing Institute of Geology and Palaeontology (NIGP), CAS in Nanjing, China. The samples were first treated with dilute hydrochloric acid (~10% HCI) and 40% hydrofluoric acid (HF) to remove carbonates and silica, and then sieved with a 10 μm nylon sieve. The prepared pollen and spores were mounted on thin slides with phenol-glycerin jelly, sealed with wax, and examined and photographed on a Zeiss Axio Scope A1 microscope with an AxioCam HRc digital camera system at NIGP. All palynological slides are deposited in NIGP.

3 Results

3.1 *Zircon morphology*

The zircon grains extracted from the studied ash layer of the Huolinhe Formation in most cases exhibit euhedral to subhedral morphologies, and oscillatory zoning patterns under CL images (Figs. 2A, 3A), indicating their igneous origin. The grains are commonly 40~200 μm in length, with a length/width ratio of 1~3.5.

3.2 *SIMS*

A total of 27 zircon grains were analyzed from the sample 059-2c, but six analyses with unexpected error were discarded (Fig. 2A; Tab. 1). Since the present zircons have high common Pb content, for which the ^{204}Pb-correction method is inaccurate, we adopted the ^{207}Pb-correction method of common Pb for age calculation. The isotopic data of the remaining 21 analyses were projected on a mixing line between common ^{207}Pb/^{206}Pb and the radiogenic ^{238}U/^{206}Pb on the inverse Tera-Wasserburg Concordia diagram (Tera & Wasserburg, 1972), and yield a lower intercept U-Pb age of 125.6±1.0 Ma (MSWD=0.53; Fig. 3A), which is interpreted as the age of the crystallization of the zircons. Since the reproducibility (accuracy) of the SIMS analysis is ~1% (Li *et al.*, 2015), we consider 1.0 Ma a reasonable uncertainty of the present SIMS U-Pb age.

3.3 *LA-ICP-MS*

A total of 40 zircon grains were analyzed from the sample 059-2b (Fig. 2B; Tab. 2). Among them three analyses with high uncertainties were excluded

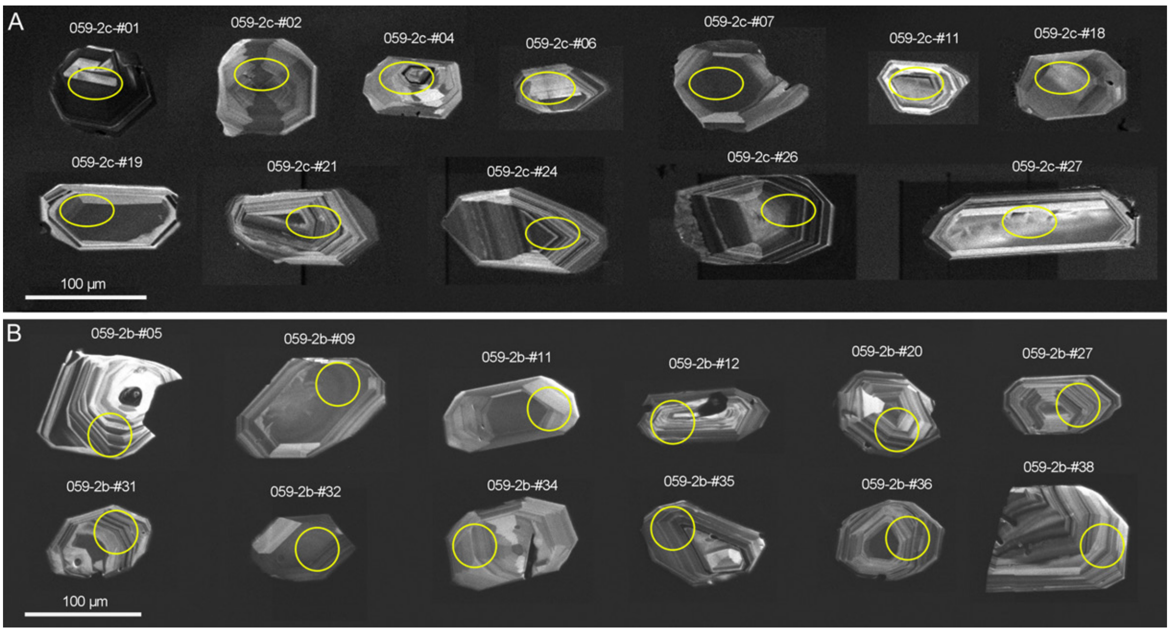

A− zircons for SIMS analyses, yellow ellipses (20 μm × 30 μm) indicating the locations of SIMS analyses. B− zircons for LA-ICP-MS analyses, the yellow rings (32 μm in diameter) indicating the locations of laser spots

Fig. 2　Representative cathodoluminescent (CL) images of analyzed zircon grains from the ash layer of the "lower coal-bearing member" of the Huolinhe Formation in Jarud Banner, eastern Inner Mongolia, China

Tab. 1 U-Pb isotopic data from SIMS analyses of zircons from the ash layer of the "lower coal-bearing member" of the Huolinhe Formation at the Zhahanaoer open-cast coal mine, Jarud Banner, eastern Inner Mongolia, China

Sample spot #	U	Th	Th/U	f_{206}%	$^{206}Pb/^{204}Pb$	Pbc uncorr. isotopic ratios				Pbc corr. isotopic ratios					Age (Ma)					
	$\times10^{-6}$	$\times10^{-6}$				$^{238}U/^{206}Pb$	$\pm\sigma$(%)	$^{207}Pb/^{206}Pb$	$\pm\sigma$(%)	$^{207}Pb/^{235}U$	$\pm\sigma$(%)	$^{206}Pb/^{238}U$	$\pm\sigma$(%)	ρ	$^{207}Pb/^{206}Pb$	$\pm\sigma$	$^{207}Pb/^{235}U$	$\pm\sigma$	$^{206}Pb/^{238}U$	$\pm\sigma$
059-2c-#01	330	198	0.601	{2.44}	767	50.056	1.53	0.06472	2.13	0.12214	8.87	0.0195	1.55	0.17484	–31.6	199.3	117.0	9.9	124.4	1.9
059-2c-#02	427	200	0.469	{0.53}	3549	51.413	1.61	0.05010	2.94	0.13437	3.35	0.0195	1.61	0.47946	199.8	66.8	128.0	4.0	124.2	2.0
059-2c-#03*	328	171	0.522	{49.91}	37	26.124	5.19	0.43457	8.06	0.09228	270.42	0.0192	9.18	0.03394	–715.9	2803.8	89.6	208.9	122.4	11.1
059-2c-#04	471	344	0.729	{0.25}	7453	49.872	1.67	0.04810	2.10	0.13299	2.68	0.0201	1.67	0.62291	104.3	48.9	126.8	3.2	128.0	2.1
059-2c-#05	265	99	0.373	{58.95}	32	19.905	1.95	0.54814	0.97	0.38473	34.90	0.0206	6.41	0.18374	2167.9	500.8	330.5	103.6	131.6	8.4
059-2c-#06	451	246	0.546	{1.35}	1382	51.130	1.58	0.05402	2.03	0.11516	6.26	0.0193	1.59	0.25457	–150.8	143.8	110.7	6.6	123.2	1.9
059-2c-#07	507	196	0.386	{0.65}	2862	50.628	1.58	0.05000	2.01	0.13617	2.56	0.0198	1.58	0.61815	195.0	46.2	129.6	3.1	126.1	2.0
059-2c-#08	581	351	0.604	{40.38}	46	31.783	2.00	0.34713	1.52	no data	no data	0.0188	2.65	no data	no data	no data	no data	no data	119.8	3.2
059-2c-#09	439	179	0.407	{20.48}	91	41.081	1.78	0.18826	3.41	no data	no data	0.0194	2.17	no data	no data	no data	no data	no data	123.6	2.7
059-2c-#10*	195	142	0.726	{0.90}	2082	56.155	1.71	0.04998	3.21	0.12271	3.64	0.0178	1.71	0.46982	193.9	73.0	117.5	4.0	113.8	1.9
059-2c-#11	164	72	0.440	{4.38}	427	48.660	1.72	0.08751	2.69	0.14417	14.15	0.0196	1.88	0.13273	337.9	290.0	136.8	18.3	125.4	2.3
059-2c-#12*	549	241	0.440	{1.22}	1536	54.127	2.60	0.05285	2.12	0.10871	8.54	0.0183	2.52	0.29570	–155.9	191.2	104.8	8.5	116.6	2.9
059-2c-#13	623	330	0.529	{79.91}	23	10.323	7.58	0.68975	1.87	0.29391	74.54	0.0195	10.12	0.13570	1791.6	954.2	261.6	188.4	124.3	12.5
059-2c-#14*	383	270	0.704	{8.18}	229	49.980	1.71	0.10850	2.30	0.11069	16.90	0.0184	1.87	0.11075	–127.7	370.2	106.6	17.2	117.4	2.2
059-2c-#15*	693	587	0.847	{30.39}	62	37.230	2.06	0.26263	11.55	no data	no data	0.0187	3.59	no data	no data	no data	no data	no data	119.4	4.3
059-2c-#16	345	179	0.518	{58.30}	32	22.896	2.13	0.49948	1.32	0.07401	112.66	0.0182	3.94	0.03499	–1213.6	1910.2	72.5	75.9	116.3	4.5
059-2c-#17	328	214	0.651	{82.61}	23	13.979	3.12	0.63478	1.47	no data	no data	0.0124	13.43	no data	no data	no data	no data	no data	79.7	10.6
059-2c-#18	322	159	0.495	{0.58}	3210	51.233	1.62	0.05084	2.39	0.13682	2.89	0.0195	1.62	0.56050	233.5	54.2	130.2	3.5	124.6	2.0
059-2c-#19	369	209	0.566	{0.08}	22721	51.333	1.61	0.04827	2.31	0.12966	2.81	0.0195	1.61	0.57071	112.7	53.6	123.8	3.3	124.4	2.0
059-2c-#20	312	275	0.880	{90.45}	21	7.713	4.57	0.73193	1.29	no data	no data	0.0124	15.23	no data	no data	no data	no data	no data	79.3	12.0
059-2c-#21	350	220	0.629	{0.39}	4757	50.628	1.61	0.04991	3.23	0.13592	3.61	0.0198	1.61	0.44675	190.8	73.4	129.4	4.4	126.1	2.0
059-2c-#22	290	95	0.326	{87.14}	21	8.573	2.85	0.71827	0.80	no data	no data	0.0150	9.56	no data	no data	no data	no data	no data	96.0	9.1
059-2c-#23	313	127	0.405	{63.62}	29	18.594	1.52	0.56617	0.79	0.25647	34.84	0.0196	4.10	0.11772	1529.2	540.7	231.8	74.9	124.9	5.1
059-2c-#24	379	305	0.804	{24.05}	78	37.773	1.57	0.24255	1.06	0.15189	23.69	0.0201	2.11	0.08925	403.4	456.3	143.6	32.2	128.3	2.7
059-2c-#25*	403	199	0.492	{53.07}	35	24.092	7.07	0.44802	4.21	no data	no data	0.0195	10.71	no data	no data	no data	no data	no data	124.4	13.2
059-2c-#26	300	152	0.505	{0.90}	2075	50.969	1.62	0.05597	2.37	0.13104	6.55	0.0194	1.64	0.25106	142.1	142.4	125.0	7.7	124.1	2.0
059-2c-#27	425	560	1.316	{0.36}	5129	49.938	1.62	0.05117	2.04	0.13287	3.64	0.0200	1.62	0.44591	114.0	75.1	126.7	4.3	127.4	2.0

Data of the samples with * were excluded from the age calculation.

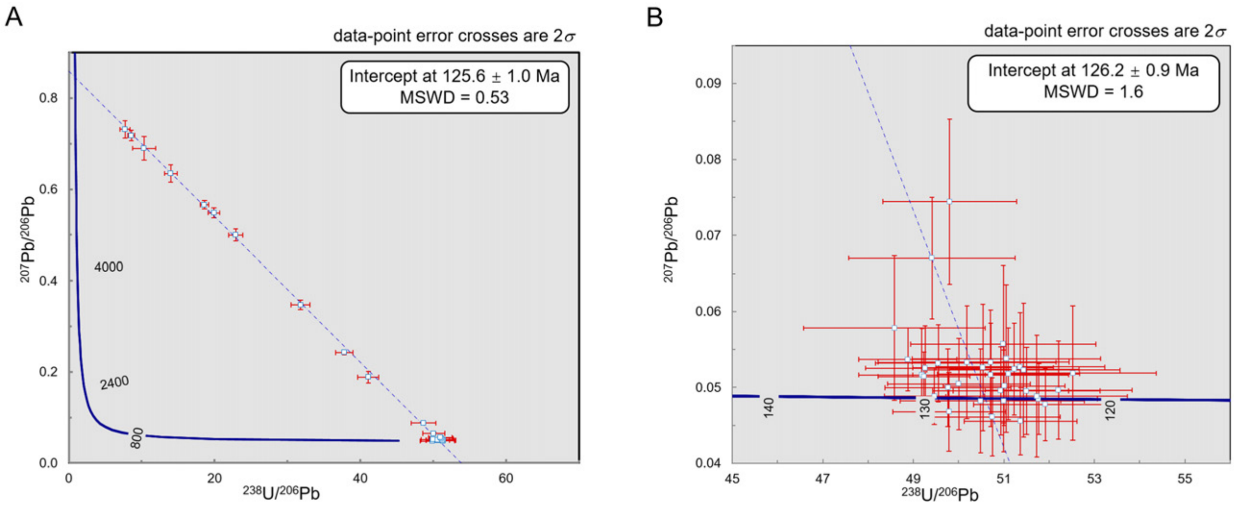

A− SIMS U-Pb zircon data; B− LA-ICP-MS U-Pb zircon data

Fig. 3　Tera-Wasserburg plots for U-Pb zircon ages of the ash layer of the "lower coal-bearing member" of the Huolinhe Formation in Jarud Banner, eastern Inner Mongolia, China

from the age calculation (Tab. 2). Three analyses with distinct older ages were interpreted as clastic grains (Tab. 2). The remaining 34 analyses yield a lower intercept U-Pb age of 126.2±0.9 Ma (MSWD = 1.6; Fig. 3B) in the Tera-Wasserburg plot. However, although the internal error of LA-ICP-MS zircon U-Pb dating can be less than 1%, the reproducibility (accuracy) of the technique is relatively poor and is ~4% (Li *et al*., 2015). This indicates that uncertainty of the present LA-ICP-MS U-Pb age could be ~5 Ma.

3.4　*Palynological assemblage*

Among the six samples only samples 059-2 (ash layer), 059-3 and 059-5 were productive for pollen and spores (Tab. 3; Figs. 4, 5). The palynological assemblage of the ash layer is diverse and includes 54 taxa. Gymnosperm pollen dominates the assemblage, with a total percentage of 54.5% and 21 taxa; spores of pteridophytes and bryophytes account for 45.1% of the assemblage, but they are more diverse with 32 taxa. Angiosperm pollen is very rare (0.4%), and represented by only *Clavatipollenites hughesii*. Gymnosperm pollen is dominated by bisaccate pollen of conifers, which accounts for approximately half of the gymnosperm component, and also includes monosulcate pollen of cycadophytes and ginkgophytes, and inaperturate pollen of Cupressaceae *sensu lato*. Among the diverse spores of pteridophytes and bryophytes, those of probable Lygodiaceae and Schizaeaceae are most common. The palynological assemblages from samples 059-3 and 059-5 are similar in composition to the assemblage from the ash layer (Tab. 3), and thus these three assemblages can be discussed together.

4　Discussion

4.1　*Palynostratigraphic analysis*

In general the palynological assemblages characterized by abundant gymnosperm pollen and diverse spores of pteridophytes and bryophytes is typical for palynofloras from the Early Cretaceous of North China (Song, 1986). Some typical Cretaceous elements including *Cicatricosisporites*, *Concavissimisporites*, *Densoisporites*, *Impardecispora*, *Jiaohepollis* and *Pilosisposrites* are very common in the assemblage, but are absent or almost absent in strata older than Cretaceous in age. These taxa are rare and low in diversity in early Early Cretaceous assemblages, and become more common and abundant in the late Early Cretaceous assemblages. In addition, monocolpate angiosperm grains resembling *Clavatipollenites* first appeared in the Valanginian–Hauterivian of the paleoequatorial regions (Friis *et al*., 2011). In middle and high latitude regions of the northern hemisphere, however, the earliest appearance of *Clavatipollenites* is later, commonly in the Barremian (Song, 1986; Zhang, 1999). In the palynomorph assemblage from the ash layer, *Clavatipollenites* is very rare. Tricolpate pollen, which typically is first recorded at around the Barremian-Aptian boundary, is absent from the samples studied so far from the Zhahanaoer open-cast coal mine, suggesting most likely a Barremian age for the palynological assemblages.

Tab. 2　U-Pb isotopic data from LA-ICP-MS analyses of zircons from the ash layer of the "lower coal-bearing member" of the Huolinhe Formation at the Zhahanaoer open-cast coal mine, Jarud Banner, eastern Inner Mongolia, China

Sample spot #	Pb	Th	U	Th/U	Isotopic ratios						Age (Ma)					
	$\times10^{-6}$	$\times10^{-6}$	$\times10^{-6}$		$^{207}Pb/^{206}Pb$	±σ	$^{207}Pb/^{235}U$	±σ	$^{206}Pb/^{238}U$	±σ	$^{207}Pb/^{206}Pb$	±σ	$^{207}Pb/^{235}U$	±σ	$^{206}Pb/^{238}U$	±σ
059-2b-#01	29.9	187.7	573.9	0.33	0.0516	0.0034	0.1395	0.0086	0.0197	0.0003	333	152	133	8	126	2
059-2b-#02	303.0	2321.6	2335.1	0.99	0.0537	0.0021	0.1516	0.0056	0.0205	0.0002	367	55	143	5	131	1
059-2b-#03	136.0	1098.6	1661.0	0.66	0.0485	0.0023	0.1299	0.0062	0.0193	0.0002	124	113	124	6	123	2
059-2b-#04	64.3	524.0	1080.8	0.48	0.0461	0.0026	0.1245	0.0064	0.0197	0.0003	400	–268	119	6	126	2
059-2b-#05	58.9	429.5	798.1	0.54	0.0527	0.0036	0.1391	0.0089	0.0195	0.0004	317	156	132	8	124	2
059-2b-#06	30.1	221.5	644.9	0.34	0.0526	0.0042	0.1447	0.0109	0.0198	0.0003	322	181	137	10	126	2
059-2b-#07	38.4	335.2	585.4	0.57	0.0519	0.0044	0.1357	0.0106	0.0190	0.0003	280	193	129	9	122	2
059-2b-#08	43.6	287.9	903.8	0.32	0.0518	0.0030	0.1370	0.0071	0.0196	0.0003	276	103	130	6	125	2
059-2b-#09	44.1	370.6	691.2	0.54	0.0482	0.0034	0.1284	0.0083	0.0196	0.0003	109	156	123	7	125	2
059-2b-#10	69.9	548.5	954.7	0.57	0.0505	0.0030	0.1384	0.0082	0.0200	0.0003	217	139	132	7	128	2
059-2b-#11	27.2	204.9	523.0	0.39	0.0488	0.0040	0.1280	0.0085	0.0193	0.0004	139	185	122	8	123	2
059-2b-#12	37.8	274.2	572.2	0.48	0.0533	0.0037	0.1436	0.0093	0.0199	0.0004	343	162	136	8	127	2
059-2b-#13	35.8	290.4	511.7	0.57	0.0523	0.0044	0.1369	0.0102	0.0194	0.0004	298	190	130	9	124	3
059-2b-#14	75.1	572.0	1181.8	0.48	0.0502	0.0026	0.1348	0.0066	0.0196	0.0003	211	120	128	6	125	2
059-2b-#15	59.1	361.4	658.9	0.55	0.0670	0.0040	0.1876	0.0114	0.0202	0.0004	839	129	175	10	129	2
059-2b-#16	18.9	147.4	448.7	0.33	0.0538	0.0049	0.1414	0.0110	0.0196	0.0004	361	206	134	10	125	3
059-2b-#17*	27.3	198.8	367.6	0.54	0.0583	0.0062	0.1406	0.0111	0.0190	0.0004	543	233	134	10	122	3
059-2b-#18*	60.5	408.6	1124.8	0.36	0.0492	0.0026	0.1452	0.0074	0.0216	0.0003	167	122	138	7	138	2
059-2b-#19	20.9	140.5	448.3	0.31	0.0578	0.0048	0.1593	0.0112	0.0206	0.0004	524	181	150	10	131	3
059-2b-#20	70.1	580.2	1000.5	0.58	0.0496	0.0029	0.1321	0.0072	0.0196	0.0003	172	137	126	6	125	2
059-2b-#21*	27.6	244.9	350.4	0.70	0.0481	0.0049	0.1200	0.0106	0.0182	0.0004	102	222	115	10	116	2
059-2b-#22*	82.2	641.7	975.1	0.66	0.0510	0.0030	0.1426	0.0076	0.0208	0.0003	243	135	135	7	133	2
059-2b-#23	170.8	1252.4	2773.4	0.45	0.0488	0.0019	0.1357	0.0050	0.0202	0.0002	139	89	129	4	129	1
059-2b-#24	61.9	431.0	1173.3	0.37	0.0532	0.0025	0.1470	0.0069	0.0202	0.0003	345	105	139	6	129	2
059-2b-#25	49.6	374.5	983.7	0.38	0.0495	0.0029	0.1307	0.0072	0.0194	0.0003	172	135	125	6	124	2
059-2b-#26*	59.9	409.1	921.1	0.44	0.0545	0.0032	0.1583	0.0087	0.0213	0.0004	394	133	149	8	136	2
059-2b-#27	36.3	251.6	792.2	0.32	0.0533	0.0034	0.1413	0.0078	0.0197	0.0003	343	146	134	7	126	2
059-2b-#28	72.2	524.7	1064.1	0.49	0.0468	0.0026	0.1288	0.0069	0.0201	0.0003	39	126	123	6	128	2
059-2b-#29	38.5	229.2	519.7	0.44	0.0744	0.0054	0.2066	0.0143	0.0201	0.0003	1054	148	191	12	128	2
059-2b-#30*	18.7	133.7	310.9	0.43	0.0626	0.0064	0.1623	0.0134	0.0198	0.0004	694	218	153	12	127	3
059-2b-#31	55.8	375.6	969.4	0.39	0.0525	0.0028	0.1469	0.0078	0.0203	0.0003	309	122	139	7	130	2
059-2b-#32	75.8	587.4	1170.1	0.50	0.0500	0.0026	0.1368	0.0065	0.0201	0.0003	195	116	130	6	128	2
059-2b-#33	82.5	654.9	1364.8	0.48	0.0478	0.0024	0.1262	0.0062	0.0193	0.0003	87	124	121	6	123	2
059-2b-#34	39.1	277.5	622.8	0.45	0.0482	0.0034	0.1307	0.0077	0.0198	0.0004	109	224	125	7	126	2
059-2b-#35	101.1	868.5	1469.0	0.59	0.0455	0.0022	0.1223	0.0059	0.0195	0.0002	-	-	117	5	124	1
059-2b-#36	51.4	340.6	1193.0	0.29	0.0517	0.0031	0.1422	0.0077	0.0203	0.0003	333	169	135	7	130	2
059-2b-#37	234.4	1787.5	4026.5	0.44	0.0514	0.0016	0.1449	0.0047	0.0203	0.0002	261	72	137	4	130	1
059-2b-#38	41.7	305.2	847.3	0.36	0.0524	0.0030	0.1402	0.0076	0.0195	0.0003	302	131	133	7	125	2
059-2b-#39	54.0	468.3	444.9	1.05	0.0557	0.0052	0.1451	0.0122	0.0196	0.0004	439	209	138	11	125	2
059-2b-#40	31.6	242.2	884.9	0.27	0.0496	0.0032	0.1298	0.0077	0.0192	0.0003	189	152	124	7	122	2

Data of the samples with * were excluded from the age calculation.

Tab. 3　Compositions and statistics of the palynological assemblages from samples 059-2 (ash layer), 059-3 and 059-5 collected from the "lower coal-bearing member" of the Huolinhe Formation at the Zhahanaoer open-cast coal mine, Jarud Banner, eastern Inner Mongolia, China

	Species	Samples		
		059-2 (%)	059-3 (%)	059-5 (%)
Spores	*Aequitriradites* sp.		0.5	
	Apiculatisporites sp.	0.4	1.1	
	Baculatisporites sp.	1.2	0.5	1.4
	Biretisporites spp.	2.7	2.6	1.4
	Cibotiumspora spp.	0.4	0.5	
	Cicatricosisporites minor	0.8	0.5	
	Cicatricosisporites spp.	1.6	1.6	1.4
	Concavissimisporites sp.	0.4		
	Contignisporites cooksonii	1.2		
	Converrucosisporites sp.	0.4	0.5	
	Cooksonites sp.		1.1	
	Crybelosporites stylosus			2.8
	Cyathidites sp.	2.7	4.2	4.8
	Cyclogranisporites sp.	1.2	1.1	
	Deltoidospora spp.	4.7	2.6	0.7
	Densoisportites velatus	1.6	1.1	2.8
	Divisisporites sp.	0.4		
	Foraminisporis wonthaggiensis		0.5	
	Gleichenidites sp.	0.4	0.5	
	Granulatisporites spp.	0.4		
	Hsuisporites sp.	0.4		
	Impardecispora apivurrucata	0.8	1.1	
	Laevigatosporites sp.	2.3	1.1	1.4
	Leptolepidites sp.	0.4		
	Lophotriletes sp.	0.4		0.7
	?*Brochotriletes*	0.4		2.1
	Lycopodiumsporites spp.	0.8	1.6	1.4
	Lygodioisporites sp.		0.5	
	Lygodiumsporites sp.		0.5	0.7
	Neoraistrickia spp.	0.4	0.5	
	Osmundacidites sp.	6.6	4.7	3.4
	Pilosisporites trichopapillosus	0.8	1.1	
	Plicifera sp.	1.2	0.5	
	Punctatisporites sp.		3.2	
	Punctatosporites sp.	1.2		
	Stereisporites psilatus	7.0	0.5	1.4
	*Todisporites*spp.	1.2	0.5	1.4
	Toroisporis sp.	0.4	0.5	
	Triporoletes sp.		1.6	
	Verrucosisporites sp.	0.8		
Gymnosperm pollen	*Abietineaepollenites* spp.	1.9	2.6	1.4
	Alisporites spp.	23.3	23.7	32.4
	Cedripites sp.	1.9	4.7	2.8
	Cerebropollenites sp.	0.8		
	Jiaohepollis verus	0.4		
	Paleoconiferus sp.	0.8		
	Parcisporites parvisaccus	0.4		
	Parvisaccites sp.	0.8		0.7
	Piceapollis sp.	8.2	2.6	2.8

continued

Species		Samples		
		059-2 (%)	059-3 (%)	059-5 (%)
Gymnosperm pollen	*Piceites* sp.	0.4	0.5	
	Podocarpidites spp.	0.4	2.1	3.4
	Pristinuspollenites sp.			0.7
	Protopicea cerina	0.8	2.1	
	Pseudopicea variabiliformis	3.5	4.7	
	Pseudopicea sp.	3.1	9.5	9.0
	Quardraeculina sp.		0.5	
	Chasmatosporites sp.		1.1	
	Classopollis classoides		0.5	
	Classopollis spp.	1.2		
	Concentrisporites		0.5	
	Cycadopites spp.	2.7	2.1	2.8
	Eucommiidites troedsonii			0.7
	Inaperturopollenites	1.6	2.6	4.8
	Monosulcites granulatus	0.8	1.1	3.4
	Perinopollenites elatoides	0.8	1.1	5.5
	Spheripollenites spp.	0.4		0.7
	Taxodiaceaepollenites hiatus	0.4	1.1	0.7
Angiosperm pollen	*Clavatipollenites hughesii*	0.4		0.7
Total grains		257	190	145

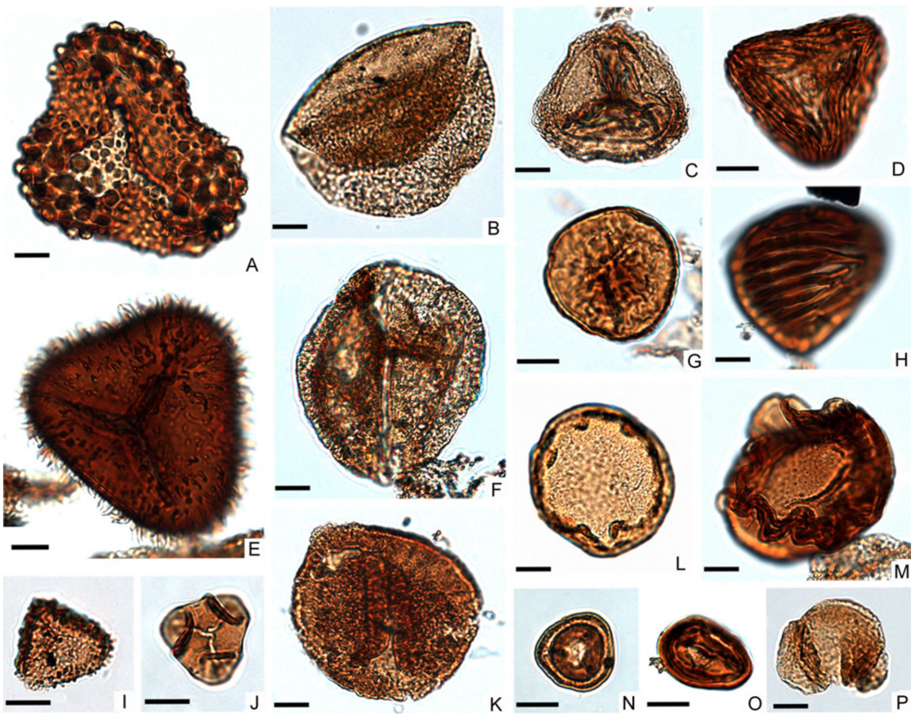

A– *Impardecispora apivurrucata* (Couper) Venkatachala; B– *Alisporites* sp.; C– *Densoisporites velatus* Weyland et Krieger; D– *Cicatricosisporites minor* (Bolkhovitina) Pocock; E– *Pilosisporites trichopapillosus* (Thiergart) Delcourt et Sprumont; F– *Protoconiferus funarius* (Naumova) Bolkhovitina; G– ?*Brochotriletes*; H– *Contignisporites cooksonii* (Balme) Dettmann; I– *Lophotriletes* sp.; J– *Cibotiumsporites juncta* (K.-M.) Zhang; K– *Cedripites* sp.; L– *Parcisporites parvisaccus* Song et Zheng; M– *Jiaohepollis verus* Li; N, O– *Classopollis* spp.; P– *Abietineaepollenites* sp. All scale bars = 10 μm

Fig. 4 Light micrographs of pollen and spores from the "lower coal-bearing member" of the Huolinhe Formation in the studied section of Jarud Banner, eastern Inner Mongolia, China

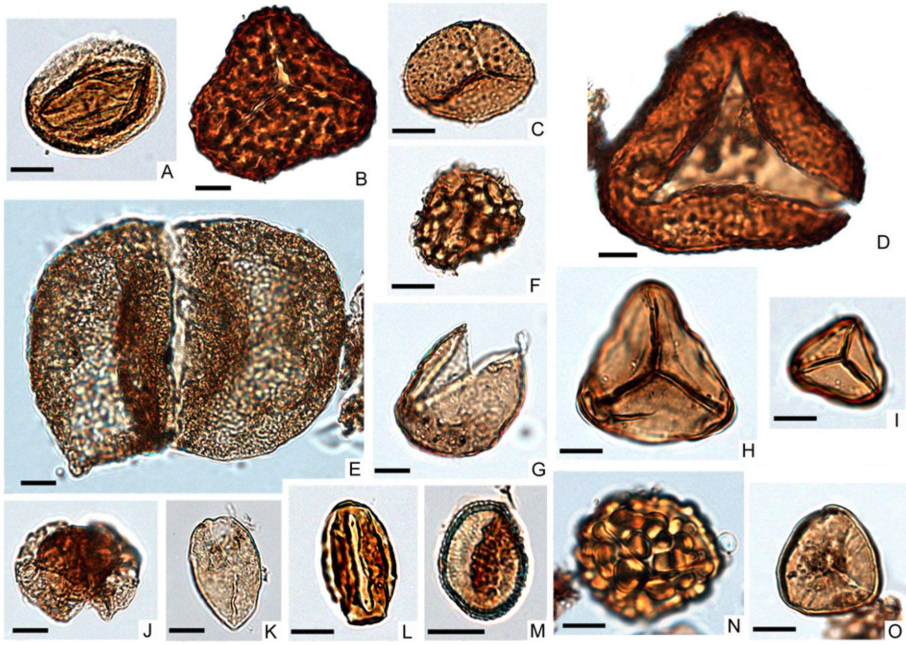

A– *Crybelosporites stylosus* Dettmann; B– *Converrucosisprites* sp.; C– *Osmundacidites welmanii* Couper; D– *Concavissimisporites* sp.; E– *Piceites* sp.; F– *Lycopodiumsporites* sp.; G– *Taxodiaceaepollenites hiatus* (Potonié) Kremp; H– *Plicifera* sp.; I– *Biretisporites* sp.; J– *Podocarpidites* sp.; K– *Cycadopites nitidus* (Balme) Pocock; L– *Eucommidites troedsonii* (Erdtman) Potonié; M– *Clavatipollenites hughesii* Couper; N– *Leptolepidites* sp.; O– *Stereisporites psilatus* (Ross) Pflug. All scale bars = 10 µm

Fig. 5　Light micrographs of pollen and spores from the "lower coal-bearing member" of the Huolinhe Formation in the studied section of Jarud Banner, in eastern Inner Mongolia, China

4.2　*Age of the Huolinhe Formation*

The U-Pb zircon age of the ash layer of the Huolinhe Formation from the SIMS analyses (125.6±1.0 Ma) is generally consistent with that from the LA-ICP-MS analyses (126.2±0.9 Ma), and both are consistent with the age inference based on palynostratigraphic analysis. All the evidence currently available suggests that the depositional age of the ash layer is late Barremian–earliest Aptian.

Guo (1995) investigated the palynomorphs from the "lower coal-bearing member" of the Huolinhe Formation at the very large South Open-cast Mine from the Huolinhe Basin ~10 km northeast of the Zhahanaoer mine. These palynomorphs are characterized by the *Cicatricosisporites*-*Pilosisporites*-*Osmundacidites* assemblage. Gymnosperm pollen (57.4%) dominates the assemblage, followed by the spores of pteridophytes and bryophytes (40.8%). Angiosperm pollen accounts for 0~2.0% of the assemblage and includes *Clavatipollenites*, *Asteropollis* and *Tricolpites* (Guo, 1995). The greater diversity and abundance of angiosperm pollen, including the presence of tricolpate eudicot pollen, suggests that the depositional age of the palynological assemblage from the South Open-cast Mine is Aptian–Albian (125–100.5 Ma), although Guo (1995) interpreted the assemblage to be of Hauterivian to early Barremian age. The palynological assemblage of the "lower coal-bearing member" from South Open-cast Mine appears younger than that from the ash layer of the Zhahanaoer mine reported here, in which angiosperm pollen is very rare (0.4%) and includes only grains similar to *Clavatipollenites* and no tricolpates. This is consistent with our conclusion that the ash layer is near the bottom of the "lower coal-bearing member" of the Huolinhe Formation based on stratigraphic analyses and borehole data. Therefore, our results provide a maximum age for the lower part of the Huolinhe Formation that is above the ash layer. The palynological sequences through the entire formation remain to be studied.

4.3　*Early Cretaceous lignite/coal-bearing basins in Northeast China and Mongolia*

Early Cretaceous lignite/coal-bearing basins are extensively developed in Northeast China and also in adjacent Mongolia. These include Fuxin and Tiefa basins in Liaoning (Chen *et al.*, 1988), the Hailar, Erlian, Dayangshu and Huolinhe basins in eastern Inner Mongolia (Deng, 1995; Deng *et al.*, 1997), and the Choyr, Tamutsag and several other small basins in eastern and central Mongolia (Ichinnorov, 2003; Nichols *et al.*, 2006; Shi *et al.*, 2014, 2016; Wang *et al.*, 2014; Herrera *et al.*, 2015, 2017). Many of these basins include important paleobotanical localities and beds that yield abundant, diverse plant fossils, but their ages are not well constrained due to lack of associated marine deposits and volcanic beds in these basins. Stratigraphic correlations based on floristic and palynological assemblages generally refer to these lignite/coal-bearing basins as of Valanginian to Albian age, but more secure age estimates for the individual basins are lacking. The more precise U-Pb ages for the palynomorph assemblages preserved associated with the ash layer of the Huolinhe Formation, together with future investigations of the palynological sequence of the entire Huolinhe Formation would provide a more refined chronological framework for the Early Cretaceous lignite/coal- bearing basins in Northeast China and Mongolia. Such research would also be of great value for constraining the age of key fossils, including the fossil plants and fossil vertebrates preserved in these basins.

Acknowledgements

We thank HU Shu Sheng, JIANG Hui, LI Qi Jia, ZHANG Wen Fang, LU Feng Wei, and administrators and staffs of the Zhahanaoer open-cast coal mine for assistance with fieldwork in Inner Mongolia, China, FENG Li Mei for processing the palynological samples, ZHANG Hua and LIU Feng for assistance in SIMS analyses, and SONG Bo Wen and ZHENG Da Ran for helpful discussion. This work was supported by the Strategic Priority Research Program (B) of Chinese Academy of Sciences (XDB26000000), the National Natural Science Foundation of China (41790454, 41802014, 41772014), the US National Science Foundation grant DEB-1748286, and the Youth Innovation Promotion Association, CAS (2017359).

References

Chen F, Deng S. 1990. Three species of *Athrotaxites* - Early Cretaceous conifer. Geoscience, 4: 27-37 (in Chinese with English abstract).

Chen F, Meng X, Ren S, Wu C. 1988. The Early Cretaceous flora of Fuxin Basin and Tiefa Basin, Liaoning Province. Geological Publishing House, Beijing, pp. 1-180 (in Chinese with English summary).

Cui J. 1995. Studies on the fusinized-wood fossils of Podocarpaceae from Huolinhe Coalfield, Inner Mongolia, China. Acta Botanica Sinica, 37: 636-640 (in Chinese with English abstract).

Deng S. 1991. Early Cretaceous fossil plants from Huolinhe Basin in Inner Mongolia. Geoscience, 5: 147-156 (in Chinese with English abstract).

Deng S. 1995. Early Cretaceous Flora of Huolinhe Basin, Inner Mongolia, Northeast China. Beijing: Geological Publishing House.

Deng S. 1997. *Eogonocormus* - A new Early Cretaceous fern of Hymenophyllaceae from China. Australian Systematic Botany, 10: 59-67.

Deng S, Ren S, Chen F. 1997. Early Cretaceous flora of Hailar, Inner Mongolia, China. Beijing: Geological Publishing House.

Dong M, Sun G. 2012. *Ginkgo Huolinhensis* sp. nov. from the Lower Cretaceous of Huolinhe Coal Field, Inner Mongolia, China. Acta Geologica Sinica (English Edition), 86: 11-19.

Friis E M, Crane P R, Pedersen K R. 2011. Early Flowers and Angiosperm Evolution. Cambridge, UK: Cambridge University Press.

Guignard G, Yang X, Wang Y. 2019. Cuticle ultrastructure of *Baiera furcata* from Northeast China and its implication in taxonomy and paleoenvironment. Review of Palaeobotany and Palynology, 268: 95-108.

Guo C. 1995. Sporopollen from the Lower part of the Huolinhe Formation, Huolinhe Basin, Inner Mongolia and its significance. PED, 22: 37-44 (in Chinese with English abstract).

Herrera F, Shi G, Ichinnorov N, Takahashi M, Bugdaeva E, Herendeen P S, Crane P R. 2017. The presumed ginkgophyte *Umaltolepis* has seed-bearing structures resembling those of Peltaspermales and Umkomasiales. Proceedings of the National Academy of Sciences USA, 114: E2385-E2391.

Herrera F, Shi G, Leslie A B, Knopf P, Ichinnorov N, Takahashi M, Crane P R, Herendeen P S. 2015. A new Voltzian seed cone from the Early Cretaceous of Mongolia and its implications for the evolution of ancient conifers. International Journal of Plant Sciences, 176: 791-809.

Ichinnorov N. 2003. Palynocomplex of the Lower Cretaceous sediments of Eastern Mongolia. Mongolian Geoscientist, 22: 12-16.

Li Q, Li X, Liu Y, Tang G, Yang J, Zhu W. 2010. Precise U-Pb and Pb-Pb dating of Phanerozoic baddeleyite by SIMS with oxygen flooding technique. Journal of Analytical Atomic Spectrometry, 25: 1107-1113.

Li R, Li X, Wang X, Sun B. 2021. First fossil liverwort with in situ flask-shaped receptacles from the Lower Cretaceous of Inner Mongolia, China. Cretaceous Research, 119: 104684.

Li R, Sun B, Wang H, He Y, Yang G, Yan D, Lin Z. 2014. *Marchantites huolinhensis* sp. nov. (Marchantiales) - A new fossil liverwort with gemma cups from the Lower Cretaceous of Inner Mongolia, China. Cretaceous Research, 50: 16-26.

Li R, Wang X, Jin P, Ma F, Yan D, Lin Z, Sun B. 2016. Fossil liverworts from the Lower Cretaceous Huolinhe Formation in Inner Mongolia, China. Acta Geologica Sinica (English Edition), 90: 838-846.

Li S, Huang J, Yang S, Zhang X, Cheng S, Zhao G, Li D, Li G, Ding J. 1982. Depositional and structural history of the late Mesozoic Huolinhe Basin and its characteristics of coal accumulation. Acta Geologica Sinica, 3: 244-254 (in Chinese with English abstract).

Li X, Liu Y, Li Q, Guo C, Chamberlain K R. 2009. Precise determination of Phanerozoic zircon Pb/Pb age by multicollector SIMS without external standardization. Geochemistry Geophysics Geosystems, 10: Q04010.

Li X, Liu X, Liu Y, Su L, Sun W, Huang H, Yi K. 2015. Accuracy of LA-ICPMS zircon U-Pb age determination: an inter-laboratory comparison. Science China Earth Science, 58: 1722-1730.

Li X, Tang G, Gong B, Yang Y, Hou K, Hu Z, Li Q, Liu Y, Li W. 2013.

Qinghu zircon: A working reference for microbeam analysis of U-Pb age and Hf and O isotopes. Chinese Science Bulletin, 58: 4647-4654.

Liu Y, Hu Z, Gao S, Günther D, Xu J, Gao C, Chen H. 2008. *In situ* analysis of major and trace elements of anhydrous minerals by LA-ICP-MS without applying an internal standard. Chemical Geology, 257: 34-43.

Ludwig K R. 2003. User's Manual for IsoPlot 3.0. A Geochronological Toolkit for Microsoft Excel. pp. 71.

Mei M, Cui J. 1994. Analysis of coal-forming plants from underlying coal-bearing member, Huolinhe Formation, Huolinhe Coal Field, Inner Mongolia. Coal Geology of China, 6: 19-21 (in Chinese).

Nichols D J, Matsukawa M, Ito M. 2006. Palynology and age of some Cretaceous nonmarine deposits in Mongolia and China. Cretaceous Research, 27: 241-251.

Rubatto D, Gebauer D. 2000. Use of Cathodoluminescence for U-Pb Zircon Dating by Ion Microprobe: Some Examples from the Western Alps // Pagel M, Barbin V, Blanc P, Ohnenstetter D (eds.). Cathodoluminescence in Geosciences. New York: Springer-Verlag, 373-400.

Shi G, Leslie A B, Herendeen P S, Herrera F, Ichinnorov N, Takahashi M, Knopf P, Crane P R. 2016. Early Cretaceous *Umkomasia* from Mongolia: Implication for homology of corystosperm cupules. New Phytologist, 210: 1418-1429.

Shi G, Leslie A B, Herendeen P S, Ichinnorov N, Takahashi M, Knopf P, Crane P R. 2014. Whole-plant reconstruction and phylogenetic relationship of *Elatides zhoui* sp. nov. (Cupressaceae) from the Early Cretaceous of Mongolia. International Journal of Plant Sciences, 175: 911-930.

Sláma J, Košler J, Condon D J, Crowley J L, Gerdes A, Hanchar J M, Horstwood M S A, Morris G A, Nasdala L, Norberg N, Schaltegger U, Schoene B, Tubrett M N, Whitehouse M J. 2008. Plešovice zircon: A new natural reference material for U-Pb and Hf isotopic microanalysis. Chemical Geology, 249: 1-35.

Song Z. 1986. A review on the study of Early Cretaceous angiosperm pollen in China. Acta Micropalaeontologica Sinica, 3: 373-386.

Sun G. 1987. *Phoenicopsis* from NE China with discussion on its taxonomy. Acta Palaeontologica Sinica, 26: 682-688.

Sun G. 1993. *Ginkgo coriacea* Florin from Lower Cretaceous of Huolinhe, northeastern Nei Monggol, China. Palaeontographica Abteilung B, 230: 159-168.

Sun G, Lydon S J, Watson J. 2003. *Sphenobaiera ikorfatensis* (Seward) Florin from the Lower Cretaceous of Huolinhe, eastern Inner Mongolia, China. Palaeontology, 46: 423-430.

Sun G, Shang P. 1988. A brief report on preliminary research of Huolinhe coal-bearing Jurassic-Cretaceous plants and strata from eastern Inner Mongolia, China. Journal of Fuxin Mining Institute, 7: 69-76 (in Chinese with English abstract).

Tera F, Wasserburg G J. 1972. U-Th-Pb systematics in three Apollo 14 basalts and the problem of initial Pb in lunar rocks. Earth and Planetary Science Letters, 14: 281-304.

Wang L, Wan C, Sun Y. 2014. A spore-pollen assemblage from the Damoguaihe Formation in the Tamutsag Basin, Mongolia and its geological implication. Acta Geologica Sinica (English Edition), 88: 46-61.

Wiedenbeck M, Allé P, Corfu F, Griffin W L, Meier M, Oberli F, Von Quadt A, Roddick J C, Spiegel W. 1995. Three natural zircon standards for U-Th-Pb, Lu-Hf, trace element and REE analyses. Geostandards Newsletter, 19: 1-23.

Xu X, Li R, Dong C, Wang Q, Jin P, Sun B. 2013. New *Schizolepis* fossils from the Early Cretaceous in Inner Mongolia, China and its phylogenetic position. Acta Geologica Sinica (English Edition), 87: 1250-1263.

Xu X, Yang L, Sun B, Wang Y, Chen P. 2017. A new Early Cretaceous *Ginkgo* ovulate organ with associated leaves from Inner Mongolia, China and its evolutionary significance. Review of Palaeobotany and Palynology, 244: 163-181.

Zhang Y. 1999. The evolutionary succession of Cretaceous angiosperm pollen in China. Acta Palaeontologica Sinica, 38: 435-453.

Zong K, Klemd R, Yuan Y, He Z, Guo J, Shi X, Liu Y, Hu Z, Zhang Z. 2017. The assembly of Rodinia: The correlation of early Neoproterozoic (ca. 900 Ma) high-grade metamorphism and continental arc formation in the southern Beishan Orogen, southern Central Asian Orogenic Belt (CAOB). Precambrian Research, 290: 32-48.

(Associate Editor: ZHANG Hai Chun)